

CHAPTER 8

Discussion And Conclusion

8.1 Discussion

The study area is located in the Northern Taranaki Basin that lies in offshore on the western side of the North Island of New Zealand. 3D Karewa seismic survey operated by Todd Petroleum mining Company Limited under Conoco Northland Limited showed a hydrocarbon amplitude anomaly at the E- 1 Prospect (Conoco Northland Ltd., 2002-2003). This prospect zone is then confirmed based on the well logs (gamma ray, density, resistivity, sonic, porosity etc.), Karewa-1 well completion report, inversion results, attributes, and porosity maps.

The study began with well log conditioning and rock physics analysis. The logs are chosen after careful checking the reading as some logs were run using different tools. Logs are corrected for problems due to casing settings, unusual spikes, and spurious data. As shear velocity (V_s) log was available for a limited zone, a V_s log is predicted from compressional velocity (V_p) for the rest of the depth and joined together to get a complete length of V_s . A RMS porosity log is calculated as the final total porosity log using density porosity and neutron porosity logs. This total porosity log is used to estimate the effective porosity log and to predict inverted effective porosities from acoustic impedance distribution for the seismic volume.

The area of the 3D Karewa survey is approximately 122.5 square kilometres with 393 inlines and 1001 crosslines. The overall data frequency is high as the frequency bandwidth of ranges from 12 to 55Hz where the mean frequency was 30Hz. In qualitative interpretation horizons are picked to check the data polarity, to define the top of the reservoir and the seismic facies, and to constrain the boundary of the inversion process. H-4 is the top of the hydrocarbon saturated reservoir sand Mangaa C-1. Faults were interpreted to get detailed structural analysis of the study area and

divided into two sets based on the times of activity and the respective intersections of horizons.

The original time-depth relationship is required for seismic-well tie. An 'adaptive approach' is applied for seismic-well tie as checkshot data was unavailable. Sonic log integration is used for depth to time conversion in this technique. The synthetic seismogram is generated to cross-correlate with the seismic trace. A bulk shift is applied to match the synthetic to the seismic data and the shape of the cross-correlation function is evaluated to keep it symmetrical by the wavelet phase rotation.

The low frequency initial model is important to extract the well information with frequencies lower than those contained in the seismic data. The initial model for acoustic impedance was created using the well data constrained by the picked horizons. As few seismic reflections of the seismic data have been seen by using the bandpass filter (0-0-10-15 Hz), a high-cut filter is applied to the initial model and frequency analysis was set 10/15 Hz (10 Hz is the high-cut filter frequency and 15 Hz is the taper frequency). The selected time window was from 800 ms to 2500 ms.

Deterministic inversion is often referred as conventional seismic inversion. The word 'deterministic' should properly refer to a model in which predictions are determined directly through a functional (physical) relationship. In deterministic inversion the estimation is a trade-off between resolution and accuracy where there are some parameters that allow a compromise between these two requirements. Model-based deterministic inversion has constraints to prevent the impedance in the solution wandering so far from the initial model that they are geologically impossible. In this study, model-based deterministic inversion is applied between the time window 800ms and 2500ms with the phase rotated wavelet extracted from the seismic data. The hard-constraint option is used which sets the maximum allowable deviations (up and down) in impedance as a percentage of the average impedance of the constraint log. In this case 100% upper and lower percentage limits are taken because if these percentages are reduced, the constraint would be tightened. The average block size was 3 ms which sets the thickness in milliseconds for the initial equal travel-time layers of the model. Prewhitening was set to 1% as a default in Hampson-Russell software although it is the noise level that is added to the amplitude spectrum of the data before analysis. The best

result comes without prewhitening but sometimes it is needed to set to stabilize the operation. The number of iterations was set to 20 to improve the convergence.

The variety of lithology for each zone influences the porosity prediction. The inverted effective porosity for horizons is predicted from the acoustic impedance results by using the polynomial relationship of acoustic impedance and porosity logs. Acoustic impedance result affected the porosity prediction as well as the lithology prediction. Lithology is predicted based on core and well logs data at the well position. Acoustic impedance and inverted porosity estimation are used to predict lithology far from the well.

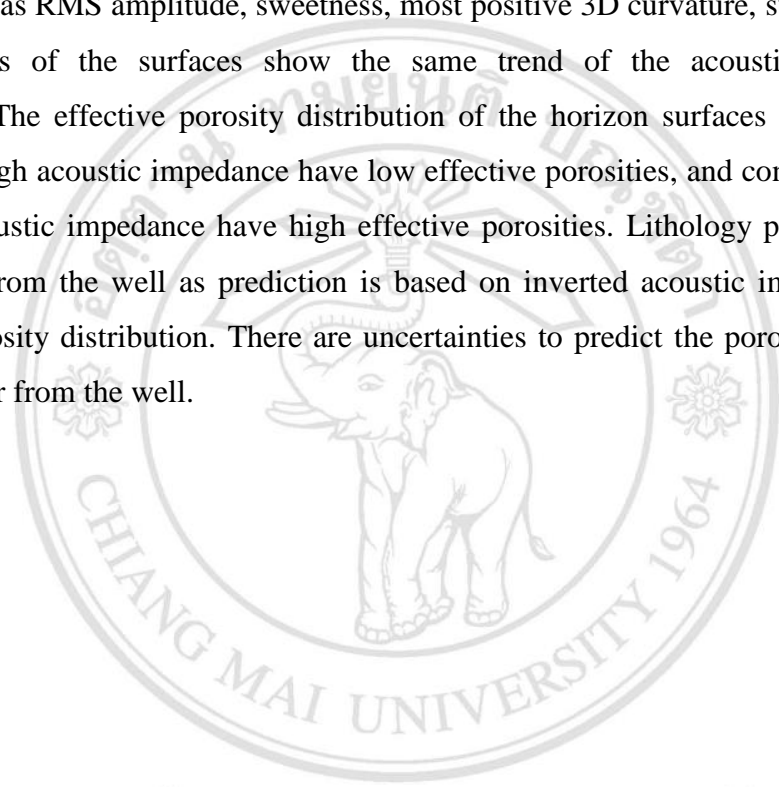
8.2 Conclusion

3D Karewa seismic data is interpreted comparatively in the deeper zone between 1119 ms and 2191 ms at the well Karewa-1 location. The highest time (TWT) interval covered by the H-1 and H-6 is 1682 ms. The seismic volume constrained by the H-1 and H-6 is divided into five units that have different amplitudes, frequencies, continuities, and configurations. One major listric type growth fault (Karewa Fault), 3 splay faults near the Karewa Fault, 13 normal faults, and one reverse fault interpreted throughout the study area shows the structural analysis. The length of the interpreted faults varies from 0.72 km (Splay Fault 1) to 10.42 km (Karewa Fault) whereas the stratal offset of interpreted faults varies from 2 to 240 ms (TWT). The orientation of faults are almost north to south except the reverse fault that has SW to NE orientation.

The model-based deterministic inversion generates broad-bandwidth frequency content that can model fine-scale heterogeneities. The acoustic impedance result from the inversion is the absolute acoustic impedance due to well log data constraint. In the inversion analysis, the RMS error (197.7) between the inverted and actual acoustic impedance is low. Moreover, the RMS correlation (0.998) is high and RMS error (0.061) is low between original seismic and synthetic. The inverted acoustic impedance ranges from 3779-8180 $((m/s)*(g/cc))$. Due to the compaction effect low values of acoustic impedance are mostly observed in the shallow depth whereas the higher values are observed in the deep zone in inversion time interval (800-2500 ms). However, low

acoustic impedance is also observed in the deep zone, for instance H-4, due to the presence of hydrocarbon.

The acoustic impedance inversion provides a straightforward conversion of seismic reflection data to the rock property, so it can be used to geological interpretation directly. The acoustic impedance distribution on horizon surfaces is extracted from the inverted acoustic impedance cube. The impedance distribution matches with attributes analysis such as RMS amplitude, sweetness, most positive 3D curvature, sweetness, etc. The attributes of the surfaces show the same trend of the acoustic impedance distribution. The effective porosity distribution of the horizon surfaces is quite well. Areas with high acoustic impedance have low effective porosities, and conversely areas with low acoustic impedance have high effective porosities. Lithology prediction was difficult far from the well as prediction is based on inverted acoustic impedance and effective porosity distribution. There are uncertainties to predict the porosities and the lithology far from the well.



ลิขสิทธิ์มหาวิทยาลัยเชียงใหม่
Copyright© by Chiang Mai University
All rights reserved